

# SENSORIAMENTO REMOTO DA ESTRUTURA DE FLORESTA USANDO LIDAR E SAR

## REMOTE SENSING OF FOREST STRUCTURE USING LIDAR AND SAR

Heiko Balzter<sup>1</sup>, Claire Burwell<sup>2</sup>, Clare S. Rowland<sup>3</sup>, Kevin Tansey<sup>4</sup>

<sup>1,2,4</sup> Centre for Environmental Research (CERES), Department of Geography, University of Leicester, University Road, Leicester, LE1 7RH, United Kingdom. <sup>3</sup> Centre for Ecology and Hydrology Monks Wood, Abbots Ripton, Huntingdon, Cambridgeshire, PE28 2LS, UK.

e-mail: <sup>1</sup> [hb91@le.ac.uk](mailto:hb91@le.ac.uk); <sup>2</sup> [clb50@le.ac.uk](mailto:clb50@le.ac.uk); <sup>3</sup> [clro@ceh.ac.uk](mailto:clro@ceh.ac.uk); <sup>4</sup> [kjt7@le.ac.uk](mailto:kjt7@le.ac.uk)

### RESUMO

As florestas desempenham um importante papel função no sistema climático global, porque absorvem e armazenam grandes quantidades de carbono sob a forma de biomassa. Este artigo analisa técnicas de recuperar a informação estrutural da floresta através de métodos de detecção remota, fazendo uso de dados LiDAR (laser) e de SAR (radar de abertura sintética). Ambos os métodos de detecção podem fornecer a informação da estrutura vertical da tipologia florestal. Determinados instrumentos LiDAR podem registrar uma forma de onda vertical da radiação refletida da floresta, cujos dados que pode ser relacionados com a distribuição vertical de biomassa. A altura da floresta é um parâmetro biofísico que é utilizado para estimar a biomassa aérea, a partir de equações alométricas. Dados SAR nos modos interferométrico e polarimétrico, de frequências distintas, podem fornecer informações sobre o modelo de elevação do terreno (DEM) sob a floresta, a altura do dossel de árvores e também, a estimativa de biomassa florestal. Os exemplos de LiDAR aerotransportado com imagem decorrentes do sistema Optech, de LiDAR orbital no modo de perfilamento (ICESAT-GLAS), de SAR interferométrico aerotransportado (E-SAR) e de SAR orbital no modo interferométrico (ALOS-PALSAR) são apresentados. Em particular, dados SAR em bandas L e X têm sido investigados para geração de mapa da altura e da biomassa da floresta, sem necessidade de um externo modelo digital do terreno. Para florestas mais densas, um comprimento de onda mais longo, tal como aqueles derivados de SAR aerotransportado em banda P torna-se necessário.

### ABSTRACT

Forests play an important role in the global climate system because they take up and store large amounts of carbon in the form of biomass. This paper examines techniques of retrieving structural forest information using the remote sensing techniques of LiDAR and SAR. Both sensing methods can provide information on the vertical structure of forests. Certain LiDAR instruments can record a vertical waveform of reflected radiation from the forest which can be related to vertical biomass distribution. Forest height is a biophysical parameter that can be used to estimate aboveground forest biomass using allometric equations. Interferometric and polarimetric SAR instruments at different wavelengths can deliver information on terrain elevation under forest, tree canopy height and biomass. Examples of airborne imaging LiDAR (Optech), spaceborne profiling LiDAR (ICESAT-GLAS), airborne interferometric SAR (E-SAR) and spaceborne interferometric SAR (ALOS-PALSAR) are presented. In particular, L-band and X-band SAR have been investigated for use to generate a forest height and biomass map without the need for an external Digital Terrain Model. For denser forests a longer wavelength such as P-band would be required.

**Keywords:** Synthetic Aperture Radar, Light Detection and Ranging, Airborne Laser Scanning, forest biomass, tree height.

## INTRODUCTION

Global forest ecosystems are vitally important in the carbon cycle, because they take up and store atmospheric carbon as a result of photosynthesis. This flux of carbon from the atmosphere to the land vegetation reduces the growth rate of atmospheric greenhouse gases caused by human impacts on the Earth system, predominantly fossil fuel burning, cement production and land use change. Despite this global importance, we have limited knowledge of the spatial distribution of forest biomass and its temporal dynamics. The processes of land use change and photosynthesis are vital for understanding the terrestrial global carbon balance. Quantitative knowledge of the biomass and hence carbon content in forest ecosystems is important for forest management, climate science and also the verification of the Kyoto Protocol and the UN Convention on Biodiversity. Forest ecosystems modify the carbon cycle through photosynthesis, heterotrophic and autotrophic respiration and disturbances including fire, windfall, insect outbreaks and logging. Considerable uncertainties remain concerning the magnitude of the carbon sink in different regions of the world and the contribution of different ecosystem processes to the global carbon cycle (SCHIMMEL et al., 2001). This illustrates the need for spatial information on the extent and amount of forest biomass. Information of this type can best be delivered from remote sensing.

The signatories of the Kyoto protocol have committed themselves to report human activities that affect their national greenhouse gas inventories from 2008-2012, with a baseline of 1990. For these reports, estimates of forest biomass changes as a result of human activities are needed. To fully understand the role of the carbon cycle in the global climate system, however, we need to go beyond the arbitrary requirements of the Kyoto protocol and develop methods for a full and all-encompassing greenhouse gas account, which includes ecosystem-atmosphere feedback mechanisms and non-anthropogenic impacts. For these purposes information on biomass and carbon stocks in forest ecosystems is needed.

Forest canopy height can be used together with allometric equations developed by forest enterprises to estimate forest biomass and carbon stocks. For example, in the UK field survey based tree top height measurements are used for estimating timber yield using a set of species-specific yield class models or non-linear functions (FORESTRY COMMISSION, 1981). It is worth defining forest canopy height, which is the height of the highest vegetation components above ground level, mean stand height, which is the mean canopy height of a forest stand, and tree height, which is the height of the tallest stem of an individual tree. Top height of a forest stand means the average total height of the 100 trees of largest diameter at breast height per hectare (FORESTRY COMMISSION, 1981). The aboveground carbon stock of a forest site can be estimated from forest canopy height and allometric equations (PATENAUDE et al., 2004).

These forestry definitions need to be considered together with remote sensing terminology to understand what information remote sensing can actually provide and to what extent it meets the expectations of the foresters. Remote sensing techniques that can be considered for this purpose include stereophotogrammetry, Light Detection and Ranging (LIDAR) and Synthetic Aperture Radar (SAR) interferometry (InSAR), including polarimetric SAR interferometry (PolInSAR). This paper will not cover stereophotogrammetry.

The principal approach of LiDAR is the transmission of near-infrared radiation (e.g. in the 1024 nm wavelength range) to the target, where the radiation is partially reflected back towards the sensor, reflected away from the sensor or absorbed. The return signal is a result of multiple interactions of the radiation with individual structural components of the target, e.g. leaves, branches, stems, undergrowth and the soil. The time the radiation takes to the target and back is measured and transformed into distance from the sensor using the speed of light as a constant. Imaging LiDAR produces spatial height maps, while profiling LiDAR produces full vertical waveforms of point locations or footprints at certain spacing along the flightline. The waveform contains a mixture of all reflected radiation components within its footprint area.

Radar operates in the microwave domain and thus the radiation interacts with water droplets contained in the target, because water has a very different dielectric constant from air. Depending on the radar wavelength and polarisation the radiation penetrates into the forest volume down to a density dependent depth where it interacts with scattering elements (leaves, stems and branches, soil). Part of the radiation is scattered back

towards the sensor and recorded. Three basic physical scattering mechanisms can be distinguished: volume scattering from multiple interactions with scatterers in the canopy, double-bounce scattering from trunk-ground interactions and rough surface scattering from the forest floor. From an interferometric image pair, a SAR interferogram can be calculated. The interferometric phase contains information on the height of the scattering phase centre, which is the vertical location within the canopy from which most of the backscatter signal is returned. The interferometric coherence indicates the degree of decorrelation between the two images. More accurate height estimates can be obtained for pixels with high coherence, because the phase error of these pixels is lower.

## AIRBORNE LASER SCANNING WITH IMAGING LIDAR

The airborne imaging LIDAR data in **Error! Reference source not found.** were acquired on 10 June 2000 by the Environment Agency over Monks Wood and Thetford forest using an Optech ALTM 1210 Airborne Laser Terrain Mapper. The coverage was one laser hit per 4.83 m<sup>2</sup> on average. The LIDAR footprint heights have a nominal accuracy of ca. 15cm, which could be confirmed in an independent comparison with Total Station GPS measurements of clear areas at Monks Wood National Nature Reserve, UK (HILL et al., 2002). The first and last return data as well as the intensity of the laser waveform were recorded for an irregularly spaced grid of points. From the last return data, a Digital Terrain Model (DTM) under the forest was interpolated under forest from LIDAR (HILL and THOMSON, 2005) with an accuracy of about 0.5m. From the first return heights a Digital Surface Model (DSM) comprised of terrain plus vegetation height was produced. The difference between the DSM and the DTM provides a Canopy Height Model (CHM) of only the vegetation layer height. The DTM had a root mean square error of  $\pm 0.51\text{m}$  and bias of  $+0.23\text{m}$  compared to theodolite data. In addition to these errors from the DTM, the CHM had a bias of  $-1.09\text{m}$  for shrubs and  $-1.95\text{m}$  for trees (HILL et al., 2002).



**Figure 1: Airborne LiDAR image of a part of Thetford forest, UK. The stands of different tree height can clearly be distinguished, and roads lined by trees are visible. LIDAR Data Copyright Environment Agency Geomatics.**

## SPACEBORNE LIDAR PROFILING WITH ICESAT-GLAS

Unlike imaging LiDAR, a profiling LiDAR transmits a pulse of radiation towards the ground and measures its returns from the first received quantum of light to the last received part of the signal. This dataset provides a full waveform for the imaged footprint. This type of LiDAR does not generate images but sets of point data, each of which contains a range of bins of values of the received radiation. An example of such a full waveform is given in Figure 2 captured over forest in Nizhnjaja Tunguska, Siberia ( $89.25^{\circ}\text{E}$  |  $65.67^{\circ}\text{N}$ ;  $89.99^{\circ}\text{E}$  |  $65.98^{\circ}\text{N}$ ), by the spaceborne ICESAT-GLAS instrument (ZWALLY et al., 2002). The part of the waveform containing the signal clearly stands out from the background noise. By isolating the thickness of the vertical layer from which the return waveform has originated we can estimate the vegetation layer height, which includes a component of microtopographic variability originating from small-scale surface elevation changes within the footprint ellipse (roughly  $60\text{m} \times 40\text{m}$ ). The vegetation layer height was estimated for 28 such LiDAR footprints over Siberian forest, selected over stands of “Forest of Natural Origin”, which is defined as “a stand of growing trees resulting from natural regeneration following a forest disturbance”. The remotely sensed vegetation height was statistically compared to forest inventory derived data (“average tree height of the dominant species in the stand”) held at the International Institute for Applied Systems Analysis

(IIASA). The results of this validation exercise are shown in Figure 3 and Table 1. While the root mean square error is quite low, a quality issue lies in the availability of footprints with a broader range of vertical values. The majority of footprints visually examined in this study showed a single spike with no layer depth information at all. It is possible that this is caused by the timing of the LiDAR data acquisition in October 2003, which is a time when dense snow covers most of the region, which could prevent vertical penetration

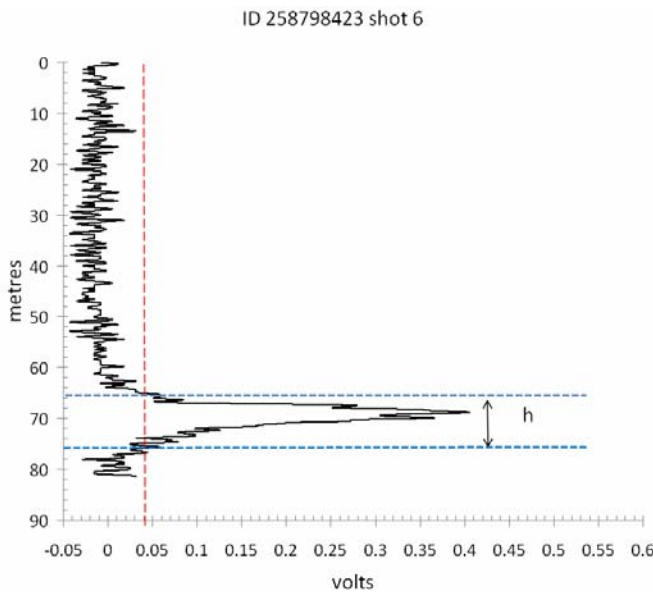


**Figure 2: Example of an ICESAT-GLAS waveform for a footprint taken over Siberia. The red line indicated the noise level that was determined empirically, and the two blue lines indicate the signal part of the waveform, which relates to the height of the vegetation layer including microtopographic variation.**

of light into the canopy. However, this has not yet been critically analysed.

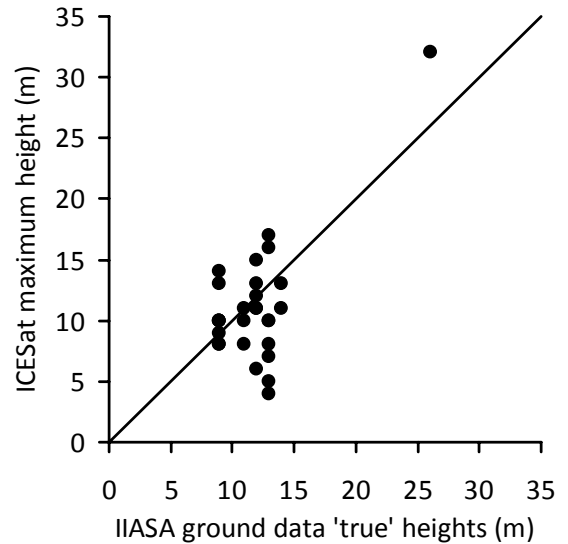


**Figure 3: Validation of ICESAT-GLAS vegetation height using “average tree height of the dominant species in the stand” from the IIASA forest inventory for land class 1101 (Forest of Natural Origin).**

**Table 1: Validation of ICESAT-GLAS vegetation height using ground data from the Russian forest inventory. The means and standard deviations of the ground data and the ICESAT-GLAS data were very similar for the 28 sample footprints, and the root mean square error was 3.77 m.**

		28 samples
<b>Ground data</b>	Mean	11.96
	Standard deviation	3.26
<b>ICESat GLAS</b>	Mean	11.14
	Standard deviation	5.13
RMSE		3.77

## AIRBORNE DUAL-WAVELENGTH SAR INTERFEROMETRY WITH E-SAR

### (i) Backscatter based approaches

The backscatter coefficient describes the energy that is received by the SAR sensor following the transmission of a microwave pulse to the target area. The three basic scattering mechanisms described earlier contribute to the backscatter coefficient at specific transmit/receive polarizations. Their magnitude depends

on the wavelength amongst other factors. Radar backscatter has been used to estimate forest biomass (LE TOAN et al., 1992) and timber volume (BALZTER et al., 2002). Mathematical models can be used to improve understanding of the interactions of the radar signal with the canopy. A water cloud model, which represents the forest as a layer of water droplets, shows that backscatter usually increases with higher forest biomass up to saturation at a certain biomass level, which depends on the radar wavelength and polarization. The saturation phenomenon limits the usefulness of SAR for forest monitoring (IMHOFF, 1995).

#### (ii) Coherence based approaches

The interferometric coherence between 2 SAR images of the same area taken from slightly different viewing positions is the magnitude of the complex correlation coefficient between the two images. The interferometric phase is the angular measurement of the same coefficient. Coherence has been found to decrease with higher forest biomass in a non-linear way as a result of volume decorrelation and temporal decorrelation. Forest stem volume was retrieved from multitemporal interferometric ERS 1 and 2 C-band tandem coherence under winter conditions over forest test sites in Finland and Sweden by ASKNE and SANTORO (2005), who conclude that the error level for large forest stands (> 2 ha) in a well managed and homogeneous boreal forest may be expected to be in the 15% to 25% range, deteriorating for small and heterogeneous stands. At L-band, multitemporal JERS-1 data showed that interferometric wintertime coherence with a 44 day temporal baseline is suitable for estimations of growing-stock volume in boreal forest in Siberia (ERIKSSON et al., 2003). TANSEY et al. (2004) present a forest growing stock classification algorithm based on the information content of both ERS tandem coherence and JERS backscatter that gives classification accuracies of greater than 70% for test sites in Sweden, Siberia and the UK.

#### (iii) Phase based approaches

The interferometric phase is related to the topographic height of the scattering phase center, which can be used to retrieve a DSM. The location of the scattering phase center within the canopy depends on vegetation structure, scattering mechanism contributions and sensor characteristics. Which scattering elements interact most strongly with the microwave radiation depends on the wavelength, polarization, incidence angle and vegetation density. Interferometric techniques can be used for estimating forest canopy height because the interferometric phase relates to the scattering phase center, which at suitable wavelengths and polarizations is composed of terrain height and vegetation canopy height (BALZTER, 2001). If there are sufficient gaps in the canopy, the interferometric height of the scattering phase center will contain a proportion from the canopy top and from the ground (HAGBERG et al., 1995). The use of interferometric SAR for estimating canopy height was demonstrated using C-band interferometric height discontinuities at forest edges by HAGBERG et al. (1995). TREUHAFT et al. (1996) carried out a modelling study for airborne C-band data and found that for an accuracy of 0.5% in the InSAR normalized cross-correlation amplitude and an accuracy of about 5° in the interferometric phase, vegetation layer depths of a few meters and ground surface heights can be estimated from interferometric SAR for many types of vegetation layers. TREUHAFT et al. (1996) found an average agreement of InSAR derived vegetation layer depth with ground data of 5 m, with the error being related to stand height. Interferometric SIR-C shuttle radar data at C- and L-band were studied over tropical rain forest by RIGNOT (1996). At L-band, the rms difference in inferred topographic height between the forest and adjacent clearings was 5 m, equivalent to the height noise (RIGNOT 1996). Repeat-pass InSAR is limited in its accuracy by temporal decorrelation caused by temperature, orientation angle and moisture changes between the two SAR acquisitions (ZEBKER and VILLASENOR, 1992; HAGBERG et al., 1995), and depends on the wavelength (ZEBKER and VILLASENOR 1992, BALZTER 2001). One approach to estimate forest canopy height is polarimetric interferometry (CLOUDE and PAPATHANASSIOU, 1998) making use of full polarimetry to estimate components of the three scattering mechanisms and their vertical locations in the canopy.

Below, we describe the production of a spatial map of forest carbon pools based on a canopy height model derived from airborne dual-wavelength SAR interferometry (see BALZTER et al., 2007, for full details). This technique was motivated by coherent microwave modelling results, which indicated that for L-band HH polarization the interferometric scattering phase center height can provide an estimate of terrain elevation under certain conditions (depending on the density and size of scattering elements in a resolution cell, ground properties, viewing geometry and moisture conditions) and the signal at X-band VV polarization if acquired

in single-pass interferometric mode can be used with certain adjustments made for penetration into the canopy as a basis to estimate mean canopy height.

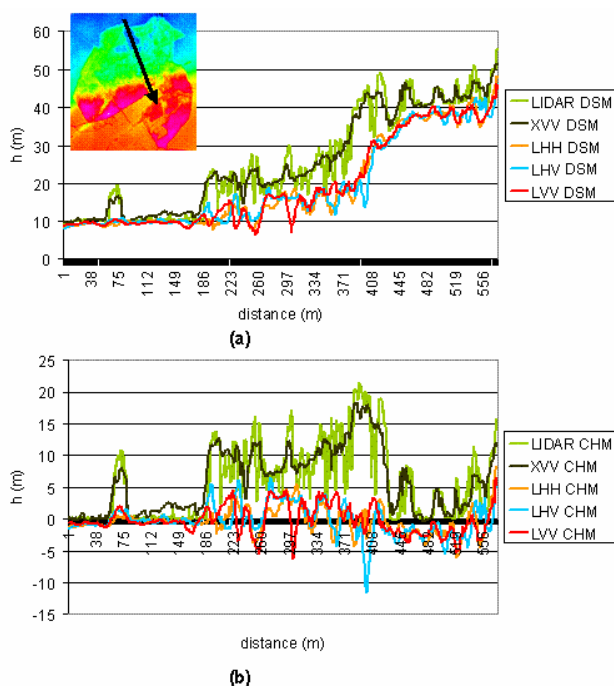


**Figure 4: Profile plots of elevation data of Monks Wood along a transect. (a) digital surface models (DSM), (b) canopy height models (CHM) derived by subtracting the LIDAR last return digital terrain model (DTM) from the DSM's in (a). The scattering phase centers at XVV are close to the LIDAR reflecting elements at the canopy top, while L-band penetrates deeper into the canopy at all polarizations. Reprinted from “Balzter, H., Rowland, C.S., and Saich, P. (2007): Forest canopy height and carbon estimation at Monks Wood National Nature Reserve, UK, using dual-wavelength SAR interferometry, Remote Sensing of Environment, 108:3, 224-239”, copyright (2007), with permission from Elsevier.**

First, DSMs were derived from the X-band VV polarized single-pass interferometric SAR data, and from the L-band HH polarized repeat-pass interferometric SAR data with a 13 minute temporal gap between acquisitions (11:21am and 11:34am). The interferometric processing involved common band filtering, interferogram generation with multi-looking (2 looks in range and 6 looks in azimuth direction), curved Earth phase trend removal, and coherence estimation with an adaptive window size between 2 and 5 and two possible weighting functions. The adaptive coherence estimation algorithm in the Gamma Interferometric SAR Processor (WEGMÜLLER and WERNER, 1997) improves the estimation accuracy of low coherence values by increasing the estimation window for pixels with low coherence and thus reducing the bias. For the coherence estimation of each pixel a corresponding window size and weighting function was selected. Then within the determined window the coherence of the central pixel was estimated as a weighted average of all pixels with local weights being related to the magnitude of the pixelwise coherence. In the case of an initial high coherence estimate of the central pixel, the coherence was estimated with a small window and areas of a high initial estimate should only contribute to the estimation process at a short distance. In the case of an initial low coherence estimate, a large window was applied. Following the coherence estimation, a phase unwrapping algorithm was applied. The flattened phase was filtered adaptively to the local slope using a Kaiser window function with a width of 6 pixels and a signal-to-noise ratio threshold of 0.2 to reduce the phase noise. Areas with coherence less than 0.25 were masked out. Phase residues were determined to avoid

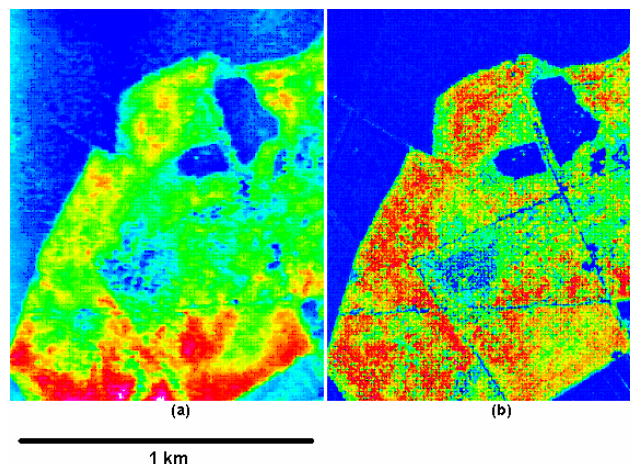


**Figure 5: Canopy height models (CHM's) of Monks Wood National Nature Reserve. (a) dual-wavelength InSAR CHM; (b) LIDAR CHM (validated using theodolite:  $rmse = 2.15$  m). Colour scale: 0...25 m. Reprinted from “Balzter, H., Rowland, C.S., and Saich, P. (2007): Forest canopy height and carbon estimation at Monks Wood National Nature Reserve, UK, using dual-wavelength SAR interferometry, Remote Sensing of Environment, 108:3, 224-239”, copyright (2007), with permission from Elsevier.**

Airborne SAR data were acquired over Monks Wood National Nature Reserve, UK, during the SAR and Hyperspectral Airborne Campaign (SHAC) on 1 June 2000 by the E-SAR sensor operated by the German Aerospace Research Institute (DLR). The E-SAR was flown in repeat-pass mode along parallel tracks at a baseline of about 10 m. L-band was acquired in quad-polarized mode (repeat-pass interferometry) and X-band in VV polarized mode (single-pass interferometry with 1.5 m baseline).

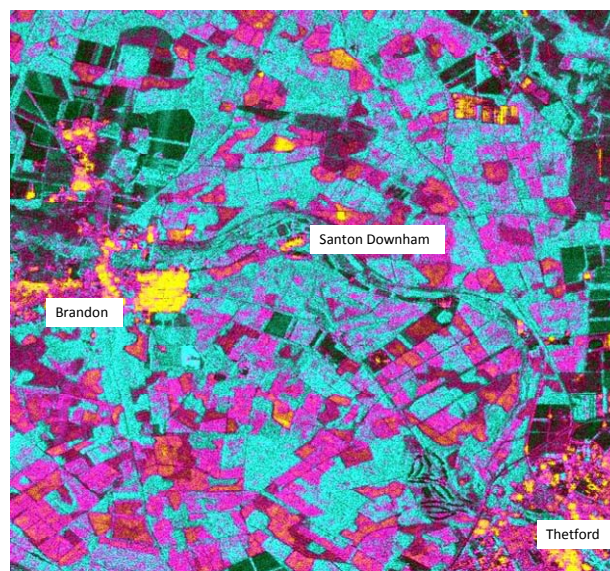
inconsistencies in the unwrapped phase image. Phase unwrapping was then performed using a region growing algorithm starting in the image center. To derive a digital elevation model unwrapped phase values were extracted for manually defined vegetation-free ground control points with known topographic height. An iterative resampling was carried out with window sizes of 7, 15 and 31 pixels to fill gaps in the ground range interferometric scattering phase center height images. All DSMs were coregistered and resampled to 3 m pixel spacing.


Figure 4 shows a transect across Monks Wood, indicating the LiDAR and SAR height values from the DSMs before and CHMs after terrain removal. It is apparent that the L-band polarizations HH, HV and VV all originate from locations near the terrain surface underneath the forest, while X-band and LiDAR both show heights near the canopy top. This allowed the retrieval of canopy height models from the two wavelengths at X- and L-band, which is presented and compared to a LiDAR derived canopy height model in Figure 5.

## SPACEBORNE RADAR MONITORING WITH MULTI-SATELLITE L-BAND SAR

There is now a long-term archive of L-band SAR data. The first civilian SAR satellite was the ocean mission SEASAT, which was launched in 1978 and operated for 105 days. The first land SAR mission at L-band was the Japanese JERS-1 which operated from 1992-1998. More recently the Japanese Space Agency launched the successor of JERS-1, the ALOS satellite with the PALSAR sensor on board. Examining multi-temporal L-band SAR backscatter has some potential for forest applications. BALZTER et al. (2003) analysed a SEASAT image and a JERS-1 image and found that the backscatter difference could be used to estimate incremental tree growth at Thetford forest, with a root mean square error of ca. 3.5 m, which decreased to 2.5 m if only forest stands greater than 2.1 hectares were considered.

Figure 6 shows an interferometric SAR image acquired by ALOS-PALSAR in 2008. A high backscatter is shown as brighter intensity in the image, while the coherence is shown as a changing hue (colour wheel). The colour representation shows mature conifer plantation forest as light blue (high backscatter, low coherence), regrowing young forest after clear felling as purple and red (medium backscatter, medium coherence), open grassland and agricultural land in black and dark green (very low backscatter, high coherence) and urban areas in yellow (high backscatter, high coherence).



**Figure 6: ALOS PALSAR interferometric image of Thetford forest, UK, 2008. Hue = coherence** , **intensity = backscatter intensity, saturation = constant. Light blue areas are mature conifer plantation forest, purple and red shades indicate regrowing young forest after clear felling, black and dark green areas are open grassland or agricultural land and yellow areas show the urban areas of Brandon, Santon Downham and Thetford.**

## CONCLUSIONS

This paper has described a range of methods for describing forest structure using both airborne and spaceborne LiDAR and SAR. While airborne methods provide the best accuracy and offer possibilities for applying better algorithms, only spaceborne data can be used relatively economically over large regions. Advanced capabilities and new sensor technology will allow for more forest structural parameters to be retrieved than were operationally mapped in the past. In the coming decade we are likely to see new remote sensing tools for forest inventory and carbon/climate research evolving from SAR and LiDAR technology.

## ACKNOWLEDGEMENTS

This work was supported by NERC under the New Observing Techniques Programme, CORSAR project, Grant number NER/Z/S/2000/01282. © E-SAR data by British National Space Centre and NERC. The UK Forestry Commission provided GIS forest inventory data. ICESAT-GLAS data were obtained from NSIDC.

## REFERENCES

- ASKNE, J.; SANTORO, M. Multitemporal repeat pass SAR interferometry of boreal forests. *IEEE Transactions on Geoscience and Remote Sensing*, 43, 1219-1228, 2005.
- BALZTER, H. Forest mapping and monitoring with interferometric synthetic aperture radar (InSAR). *Progress in Physical Geography*, 25, 159-177, 2001.
- BALZTER, H. et al. Retrieval of timber volume and snow water equivalent over a Finnish boreal forest from airborne polarimetric Synthetic Aperture Radar. *International Journal of Remote Sensing*, 23, 3185-3208, 2002.
- BALZTER, H. et al. Estimation of tree growth in a conifer plantation over 19 years from multi-satellite L-band SAR. *Remote Sensing of Environment*, 84, 184-191, 2003.
- BALZTER, H. et al. Forest canopy height and carbon estimation at Monks Wood National Nature Reserve, UK, using dual-wavelength SAR interferometry. *Remote Sensing of Environment*, 108, 224-239, 2007.
- CLOUDE, S.R.; PAPATHANASSIOU, K.P. Polarimetric SAR interferometry. *IEEE Transactions on Geoscience and Remote Sensing*, 36, 1551-1565, 1998.
- ERIKSSON, L.E.B. et al. Multitemporal JERS repeat-pass coherence for growing-stock volume estimation of Siberian forest. *IEEE Transactions on Geoscience and Remote Sensing*, 41, 1561-1570, 2003.
- FORESTRY COMMISSION. Yield models for forest management (booklet 48), Edinburgh: Forestry Commission, 1981.
- HAGBERG, J.O. et al. Repeat-Pass SAR Interferometry over Forested Terrain. *IEEE Transactions on Geoscience and Remote Sensing*, 33, 331-340, 1995.
- HILL, R.A. et al. Accuracy issues in the assessment of deciduous woodland canopy height by airborne laser scanning: a case study. ForestSAT, 5-9 August 2002, Edinburgh, Forest Research, Forestry Commission, CD-ROM, 2002.
- HILL, R.A.; THOMSON, A.G. Mapping woodland species composition and structure using airborne spectral and LiDAR data. *International Journal of Remote Sensing*, 26, 3763-3779, 2005.
- IMHOFF, M.L. Radar Backscatter and Biomass Saturation - Ramifications For Global Biomass Inventory. *IEEE Transactions on Geoscience and Remote Sensing*, 33, 511-518, 1995.
- PATENAUDE, G. et al. Quantifying forest above ground carbon content using LiDAR remote sensing. *Remote Sensing of Environment* 93, 368-380, 2004.
- LE TOAN, T. et al. Relating Forest Biomass to SAR Data. *IEEE Transactions on Geoscience and Remote Sensing*, 30, 403-411, 1992.
- SCHIMMEL, D.S. et al. Recent patterns and mechanisms of carbon exchange by terrestrial ecosystems. *Nature*, 414, 169-172, 2001.
- TANSEY, K.J. et al. Classification of forest volume resources using ERS tandem coherence and JERS backscatter data. *International Journal of Remote Sensing*, 25, 751-768, 2004.
- TREUHAFT, R.N. et al. Vegetation characteristics and underlying topography from interferometric radar. *Radio Science*, 31, 1449-1485, 1996.
- WEGMÜLLER, U.; WERNER, C. Retrieval of vegetation parameters with SAR interferometry. *IEEE Transactions on Geoscience and Remote Sensing*, 35, 18-24, 1997.
- ZEBKER, H.A.; VILLASENOR, J. Decorrelation in Interferometric Radar Echoes. *IEEE Transactions on Geoscience and Remote Sensing*, 30, 950-959, 1992.
- ZWALLY, H.J. et al. ICESat's Laser Measurements of Polar Ice, Atmosphere, Ocean, and Land, *Journal of Geodynamics* 34, 405-445, 2002.